Damage detection based on strain transmissibility for beam structure by using distributed fiber optics

Damage detection based on strain transmissibility for beam structure by using distributed fiber optics

Liangliang Cheng ,Giorgio Busca , Marcello Vanali Paolo Roberto and Alfredo Cigada*

Department of Mechanical Engineering, Politecnico di Milano, Via la Masa 1 – 20156, Milano, Italy

*Corresponding author. E-mail address:alfredo.cigada@polimi.it

ABASTRACT: Structural damage identification is a coral and challenging research topic. Research mainly focuses on identification and detection of linear damage in structures by using modal parameters such as change of natural frequency, frequency response function, mode shape, etc. Transmissibility is conventionally defined as the spectra ratio of two measurement points, which has been utilized for damage identification as a powerful damage indicator. In this paper, strain transmissibility, defined as ratio of strain response spectra, is proposed as a new damage indicator. In order to achieve more precise sensing information, distributed fiber optics has been applied to damage detection on a beam structure, which adds new capability of sensing with its combination of high spatial density sensing and dynamic acquisition over a single optical fiber sensor. A numerical simulation has been conducted to investigate the feasibility of strain transmissibility for damage detection which has revealed a better performance compared to traditional transmissibility. The applicability of the proposed method has been confirmed by applying distributed fiber optics on a clamped-clamped beam. Both simulation and experiment validate the effectiveness of damage detection approach based on strain transmissibility by using distributed fiber optics.

Key words: Strain transmissibility, distributed fiber optics, optical frequency domain reflectometer (OFDR), dynamic measurement, damage detection

1. Introduction

Most of civil, mechanical and aerospace structures are vulnerable to damage due to human factors, natural disasters, prolonged fatigue or corrosion. Therefore, in the last twenty years structural health monitoring has been extremely attractive to supervise the health status of structures. Damage detection techniques are based on a wide variety of physical principles [1], mainly focused on vibrations and modal parameters. A review work of damage detection methods based on modal parameters was carried out by Doebling et al. [3] [4] [5].

Damage detection performed on modal parameters (natural frequency, mode shape and damping) has many advantages compared to other methods mainly due to the fact that modal parameters merely depend on the characteristics of structures themselves [2]. Since structural vibration characteristics depend on structural physical parameters, a change of the physical parameters due to a damage, for instance a stiffness reduction, will inevitably cause a change of the structural dynamic response.

Modal parameters identification during a continuous monitoring is usually performed by using only output measurement data and operational modal analysis. However, this could be a troublesome point in some cases, because the a priori hypothesis about independency of the modal parameters on the excitation level and the requirement of a flat spectrum of the driving force is not always respected. Among the operational feature that can be estimated from the structure response, transmissibility function drew the attention of many researchers, because it does not require any prior knowledge of the exciting force and no modal identification is needed. Transmissibility is conventionally defined as the ratio of the spectra of two different outputs of the system and it was proposed as damage feature firstly in [6]. The damage feature is usually the difference among the transmissibility functions of the health structure and an unknown scenario. Maia et al. [7] carried out a rather comprehensive analysis about transmissibility theory and they proposed the Detection and Relative Damage Quantification Indicator (DRQ) as a reliable damage detection indicator [8].

In the papers [9], [10] and [11], the authors have worked on the extension of transmissibility concept to multiple degree freedom. It is worth mentioning that Lang et al. proposed also to extend the transmissibility to nonlinear damage detection based on NOFRF (non-linear output frequency response functions) in [12] and [13]. DRQ is calculated through evaluating integral difference over a fixed frequency band between intact transmissibility and damaged transmissibility. However, the outcomes of damage identification are extremely influenced by the choice of this frequency band as described in [14], [15] and [16]. Recently, this issue was discussed by Patrick Guillaume's papers ([17], [18]) who proved that the limit value of the transmissibility function to the poles of the system converges to the ratio of the mode shapes of the two measurement points. They also pointed out that by using only a small frequency band around the resonance frequencies of structures, the outcomes of damage identification are more reliable and independent from the force location. A detailed review of transmissibility function can be found in [20].

The accuracy of damage localisation, based on the aforementioned transmissibility function, relies on the number of sensors as well. When dynamic test is performed on large structures such as bridges, tunnels and buildings, conventional sensors are extremely difficult to cover the entire target. Usually the number of sensors needed to do this it is too big and then the idea is impracticable mainly for economic reasons. Fortunately, distributed fiber optics techniques have kept developing rather maturely and they have been applied into various domains [21], [22] and [23]. Distributed fiber optic sensors can measure continuously strain and temperature along the structure layout and in some cases they can also be embedded into concrete for checking the internal health status. Generally speaking, distributed fiber optic sensors can be classified into three categories based on Rayleigh, Brillouin and Raman scattering techniques [21] which can be chosen according to specific requirements.

This paper will report the developing of strain transmissibility function and its corresponding damage indicator by using distributed fiber optic sensor. A short review of damage detection based on traditional transmissibility function algorithm is described in section 2. In section 3, strain transmissibility has been proposed. Simulation and experiment have been discussed in section 4 and 5 respectively. The last section gives the conclusion of this paper. It will be shown that strain transmissibility function is more sensitive to damage than traditional transmissibility functions based on acceleration and displacement data. Simulations and experiments are carried out and have proved the feasibility of damage detection by using strain transmissibility function.

2. **Transmissibility functions algorithm**

Transmissibility function is traditionally defined as the ratio of two different output spectra. As for a MDOF system, let $F_k(s)$ be driving force at DOF k, then the transmissibility function $T_{ij(k)}(s)$ can be calculated as

$$T_{ij(k)}(s) = \frac{X_{ik}(s)}{X_{jk}(s)} = \frac{H_{ik}(s)F_k(s)}{H_{jk}(s)F_k(s)} \tag{1}$$

where $X_{ik}(s)$ and $X_{jk}(s)$ are the system outputs at DOF *i* and DOF *j* respectively; H_{ik} and H_{jk} are the frequency response functions at DOF *i* and DOF *j* respectively.

Similarly, transmissibility functions can also be defined in the same way between the same pair DOF i and DOF j when there is damage in the structure:

$$T^D_{ij(k)}(s) = \frac{X^D_{ik}(s)}{X^D_{jk}(s)} = \frac{H^D_{ik}(s)F_k(s)}{H^D_{jk}(s)F_k(s)} \tag{2}$$

where superscript *D* stands for the damaged status of the structure.

Johnson [22] proposed the following damage indicator based on transmissibility function:

$$DI_{ij(k)} = \left| \sum_{\omega} \left(\frac{TP^D_{ij(k)}(\omega) - TP_{ij(k)}(\omega)}{TP_{ij(k)}(\omega)} \right) \right| \tag{3}$$

where $TP_{ij(k)}(\omega) = \left|\log(T_{ij(k)}(\omega))\right|$.

Additionally, literature also proposes a damage indicator based on occurrences that seems to provide more reliable and robust results according to the authors [18]. It can be briefly explained that an occurrence is counted for each frequency step at the location where the difference between intact and damaged transmissibility is maximum. Hence, the result of occurrence relies on the frequency band that you choose. The corresponding equation is

$$O_{ij(k)}(\omega) = Count(\max_{\omega} \left|TP^D_{ij(k)}(\omega) - TP_{ij(k)}(\omega)\right|) \tag{4}$$

From equation (3), it is shown that damage element could correspond to the maximum value of damage indicator integrated over a range of frequency band. The paper also demonstrates that the integration of frequency band could be applied to a small frequency band around the resonance frequencies of the structure under different loading conditions.

The limit value of the transmissibility function equation (1), when variable s (the generic pole) approaches the system's poles, depends only on the mode shapes [7]:

$$\lim_{s \to \lambda_m} T_{ij(k)}(s) = \frac{\phi_{im}}{\phi_{jm}} \tag{5}$$

where ϕ_{im} and ϕ_{jm} are the scalar mode-shape values.

It is obvious to observe that the limit value of transmissibility function is independent from the location and nature of the force. The variable k here defines the specific loading position. Therefore, the following equation is established:

$$\lim_{s \to \lambda_m} T_{ij(k)}(s) = \lim_{s \to \lambda_m} T_{ij(l)}(s) \tag{6}$$

Damage indicator can be calculated by using the difference between intact and damage transmissibility under integrating a small range around resonance frequencies independently from the forcing location [18].

3. **Strain transmissibility function**

Usually, traditional transmissibility function (TTF) is calculated by acquiring acceleration, velocity or displacement measurement data. In this paper strain data are considered as base for a new transmissibility function, named Strain Transmissibility Function (STF). The aim of this work is to prove that STF is more sensitive to damage compared to TTF, based on the research achievement of TM Whalen, who has proved that higher order mode shape derivatives (e.g., modal curvature, third derivatives, and fourth derivatives) show better performance in terms of damage than the mode shape for beam-like structures [19].

The strain frequency response function between the loading point *k* and measurement point *i* can be written as:

$$H_{ik}^{\varepsilon}(\omega)=\frac{X_i^{\varepsilon}(\omega)}{F_k(\omega)}=\sum_{r=1}^{N}\frac{\delta_{ir}\varphi_{kr}}{M_r(\omega_r^2-\omega^2+2j\xi_r\omega_r\omega)} \tag{7}$$

where δ_{ir} and φ_{kr} are the *r*th order strain mode shape and displacement mode shape respectively while ω_r is the resonance frequency. Variable *k* and *i* represent loading point and measurement output point respectively. Then the strain transmissibility function (STF) between two strain frequency response functions becomes:

$$T_{ik}^{\varepsilon}(\omega)=\frac{H_{ik}^{\varepsilon}(\omega)}{H_{jk}^{\varepsilon}(\omega)}=\frac{\sum_{r=1}^{N}\frac{\delta_{ir}\varphi_{kr}}{M_r(\omega_r^2-\omega^2+2j\xi_r\omega_r\omega)}}{\sum_{r=1}^{N}\frac{\delta_{jr}\varphi_{kr}}{M_r(\omega_r^2-\omega^2+2j\xi_r\omega_r\omega)}} \tag{8}$$

when the variable ω approaches to the resonance frequencies ω_r, the limit value can be obtained according to STF definition equation (8).

$$\begin{aligned}\lim_{\omega\to\omega_r}T_{ik}^{\varepsilon}(\omega)&=\lim_{\omega\to\omega_r}\frac{\sum_{r=1}^{N}\frac{\delta_{ir}\varphi_{kr}}{M_r(\omega_r^2-\omega^2+2j\xi_r\omega_r\omega)}}{\sum_{r=1}^{N}\frac{\delta_{jr}\varphi_{kr}}{M_r(\omega_r^2-\omega^2+2j\xi_r\omega_r\omega)}}\\&=\lim_{\omega\to\omega_r}\left.\frac{\frac{\delta_{ir}\varphi_{kr}}{M_r(\omega_r^2-\omega^2+2j\xi_r\omega_r\omega)}}{\frac{\delta_{jr}\varphi_{kr}}{M_r(\omega_r^2-\omega^2+2j\xi_r\omega_r\omega)}}\right|_r\\&=\frac{\delta_{ir}}{\delta_{jr}}\end{aligned} \tag{9}$$

It is known that FRFs can be decomposed into SDOF in modal space. When ω approaches to resonance frequencies ω_r, the corresponding mode will dominate the whole FRF. Similar to equation (5), equation (9) demonstrates the limit value of STF in system poles is strain mode shape ratio.

Besides, it is known that the relationship between strain and bending moment according to beam's elastic theory:

$$\varepsilon=\frac{M}{EI}\cdot h_{\max} \tag{10}$$

Where *M* is the section moment, *EI* is bending stiffness, h_{max} is the distance from the measurement point to the neutral axis.

However, bending curvature has the following relationship:

$$C=\frac{1}{\rho}=\frac{M}{EI}=\frac{d^2y}{dx^2} \tag{11}$$

Where C is the curvature, $\rho$is the radius of curvature, y is the displacement normal to the neutral beam axis.

Therefore, the relationship between strain and displacement can be shown as:

$$\varepsilon=\frac{d^2y}{dx^2}\cdot h_{\max} \tag{12}$$

The dynamic displacement of beam structure at any position x and at any time t can be redefined as the product of space function and time function by applying separation variable method:

$$y(x,t)=\sum_{i=1}^{N}\phi_i(x)\eta_i(t) \tag{13}$$

Where ϕ and η are mode shape and modal coordinate respectively.

Therefore, substitute equation (13) into (12), strain can be rewritten as:

$$\begin{aligned}\varepsilon(x,t)=\frac{d^2y(x,t)}{dx^2}\cdot h_{\max} &= h_{\max}\cdot\sum_{i=1}^{N}\phi_i''(x)\eta_i(t) \\ &= h_{\max}\cdot\sum_{i=1}^{N}\delta_i(x)\eta_i(t)\end{aligned} \tag{14}$$

Where δ is strain mode shape.

According to equation (12), strain is equal to the product between the second derivative of displacement and a constant which is the distance from the measurement point to neutral axis. By combing this final statement with the conclusion proposed by TM Whalen, that second mode shape derivatives are better damage indicator compared to the mode shape in terms of beam-like structures [19], it is possible to declare that strain mode shape is more sensitive than displacement mode shape to damage. Therefore, the assumption that STF in correspondence of system's poles is more sensitive to damage than traditional TTF can be established.

4. **Simulation validation**

In order to validate the effectiveness of the proposed assumption, harmonic response analysis has been performed on a simulated beam structure. Both displacement FRFs and strain FRFs have been extracted and used to calculate TTF and STF.

4.1 Simulation model

A clamped- clamped steel beam structure has been simulated by means of the commercial software ANSYS©. The dimensions are 1.5 m × 0.04 m × 0.015 m. The beam is meshed with 25 beam elements and 26 nodes. Damage is simulated by adding a point mass (0.23kg, approximately 3% of the total mass, black block shown in Fig. 1) on element 19, which could be considered as linear damage that only changes the element mass between node 19 and node 20. Dynamic analysis is conducted for both intact and damaged beam, displacement responses and strain responses of all nodes have been acquired for both beams under two different scenarios. F1 and F2 are two impulse input forces on different node positions (node 3 and node 21 respectively) based on the fact that the intersections of two transmissibility functions on one specific measurement point under different loading situation corresponds to the natural frequencies of the system [18]. If there is damage, the intersections of those transmissibility functions are not coincidence with system's natural frequencies anymore and the damage indexes should reveal this fact.

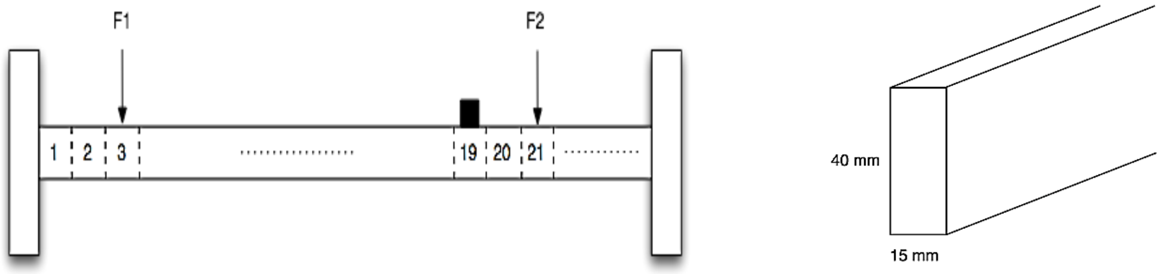

Fig. 1 The whole beam frame of FEM model and beam cross

4.2 Simulation results

F1 and F2 have been imposed on the intact beam as shown in Fig. 1 . According to equation (6), it is well known that the intersection of strain transmissibility functions under two different loading positions should be in accordance with systems' poles. Fig. 2 shows the STFs acquired from 10th beam node of the intact beam under the loadings F1(3th beam node) and F2 (21th beam node) respectively.

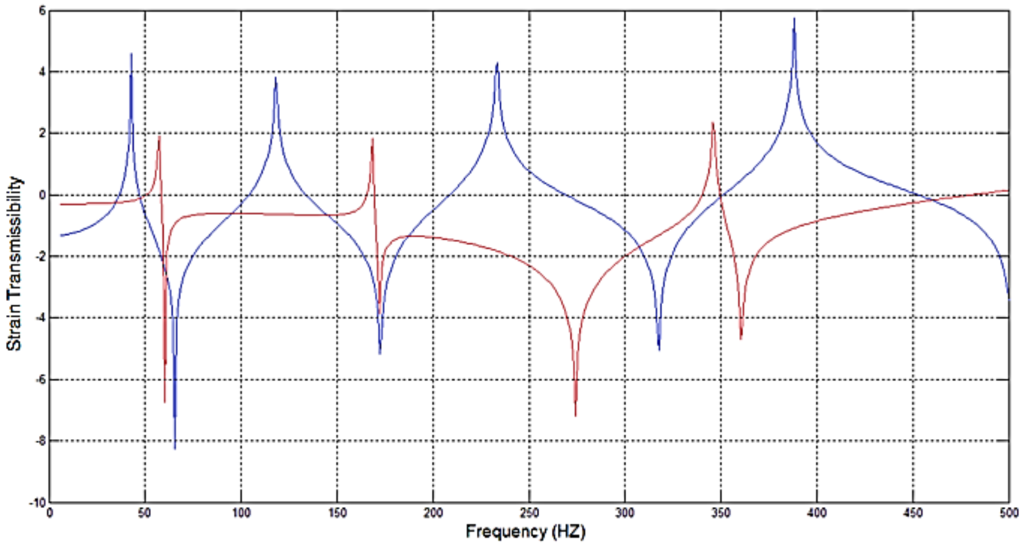

Fig. 2 10th measurement point STFs of intact beam for two different loading points

In order to locate damage properly, TTFs and STFs are estimated on pairs of consecutive measurement points to calculate both intact and damaged beam structures. Applying equations (1), (2) and (3), damage features could be obtained for TTFs and STFs. In this case, a small frequency band around the first resonance frequency of the intact beam (35Hz) is selected to calculate the damage indicators by computing the difference between intact and damaged beam structure. The frequency band is fixed between 34-36Hz around the first mode. Fig. 3 and Fig. 4 show the damage indicator DI by using TTFs and STFs respectively.

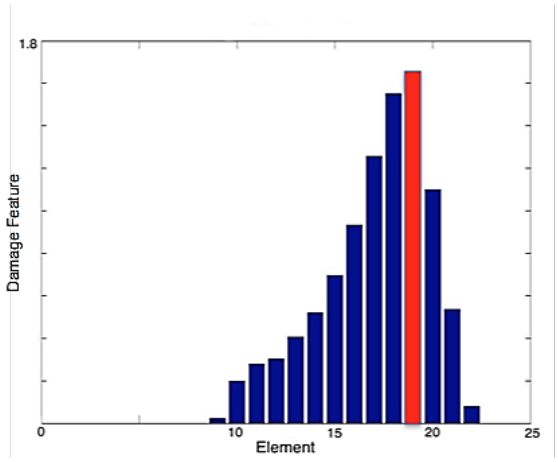

Fig. 3 Damage feature by using TTFs

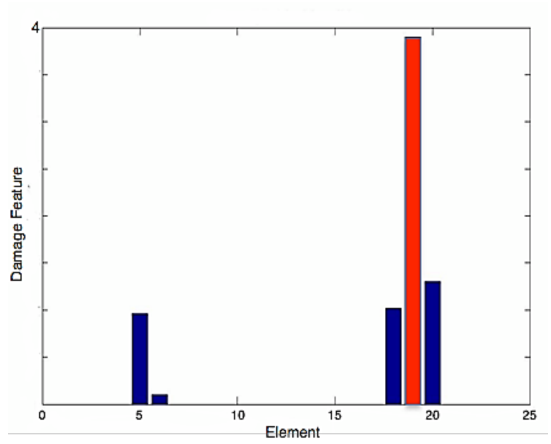

Fig. 4 Damage feature by using STFs

The red bars point out the damage location, apparently both damage indicators are able to figure out the correct damage location 19th element. One more interesting thing needs to be noticed, damage indicator calculated by STFs seems more explicit compared to the one from TTFs. Basically, the maximum damage feature could correspond to the true damage location which localizes at 19th element shown in Fig. 3, however, the difference between 18th and 19th beam element is quite small in terms of damage indicator, which might make the result ambiguous. In contrast, damage indicator by using STFs in Fig. 4 shows a very clear result since there is only one high value at the19th beam element obviously.

The simulated data were also processed by the damage feature based on occurrences to test its performance. Fig. 5 and Fig. 6 show the results from occurrences and analogous conclusions to the previous case can be drawn. Both the measurements (displacement and strain) indicate precisely the damage location. Moreover, occurrences in Fig. 6 demonstrates that STFs are more sensitive than TTFs in terms of damage detection since only one damaged bar is shown.

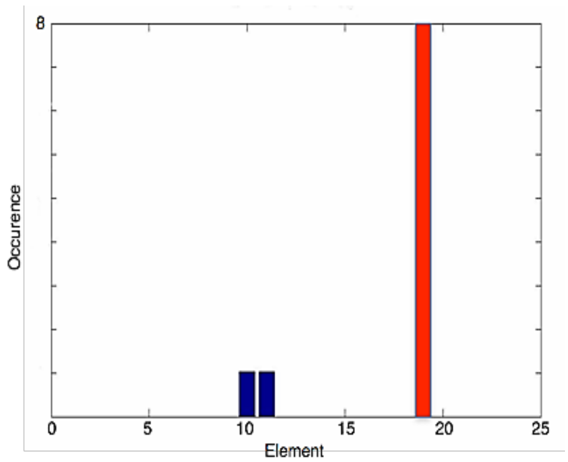

Fig. 5 Occurrence by using TTFs

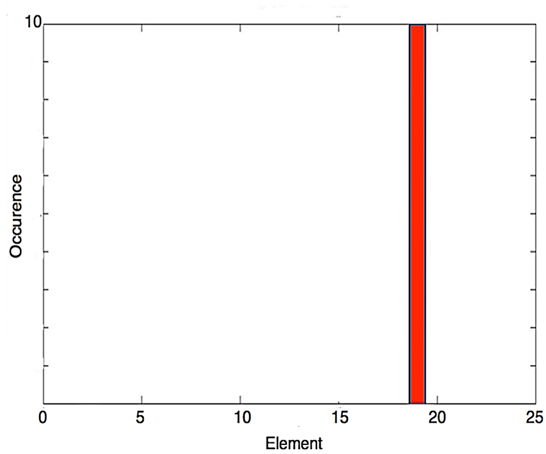

Fig. 6 Occurrence by using STFs

Apparently, occurrence is able to locate damage in a more robust and effective way, though damage indicator by using difference between intact and damaged TFs is able to work properly. Besides, no matter which the damage feature is used, it has shown that STFs have better performance on damage identification with respect to TTFs.

5. Experiment validation

Since damage localisation depends on the number of sensing points, distributed fiber optics sensor has been applied for strain measurement because it is capable to provide numerous sensing points. Therefore, LUNA ODiSI-B optical distributed sensor interrogator has been adopted; which uses optical frequency domain reflectometry technique to measure strain along one single fiber.

5.1 Brief introduction of ODiSI-B

Optical distributed sensor interrogator (Model ODiSI-B in Fig. 7) provides a paramount industrial solution for applications in many fields with outstanding spatial resolution. LUNA's ODiSI B is capable to cover more than 10 meters of dynamic measurement range with a high density of measurement points. ODiSI B can simultaneously demodulate thousands sensing points over a single optical fiber at a frequency of 100Hz. 10 m maximum sensing distance and spatial resolution of 2.56 mm make ODiSI B an extremely important tool as for strain and temperature sensing applications. Fig. 8 shows the operational interface of data acquisition software for ODiSI-B.

Fig. 7 Model ODiSI-B

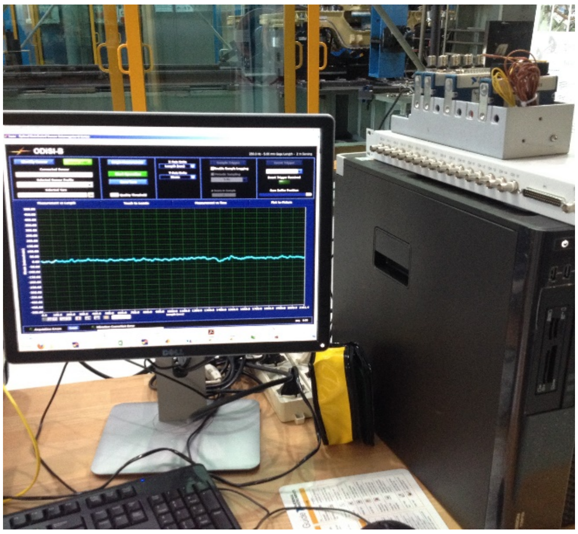

Fig. 8 Interface of DAQ system

5.2 Experimental setup

A clamped-clamped steel beam has been utilized with dimension 1.5 m × 0.04 m × 0.015 m. In order to attach the fiber optics firmly, the steel beam surfaces were polished and then a specific glue was used to attach the fiber optics as shown in Fig. 9.

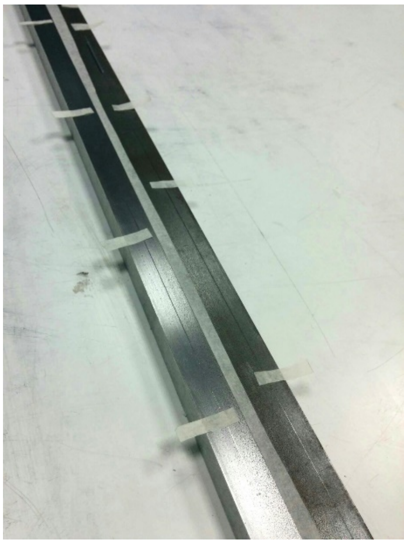

Fig. 9 Beam attached with fiber optic

Fig. 10 Beam experiment setup

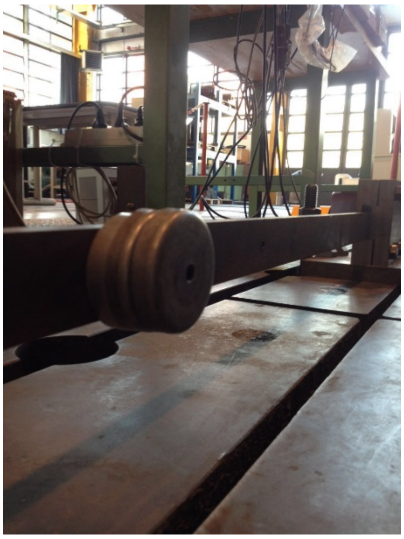

Fig. 11 Magnets added into beam

Fig. 10 shows the whole frame of beam structure. Magnets are attached to the surface of the beam in order to increase the weight of beam itself, which is able to simulate linear damage situation due to the change of dynamic characteristic (Fig. 11). The weight of the magnets is about 0.23kg over 7.1kg of the beam.

5.3 Experimental result

The fiber optic we chose is 2 meters long and covers the full length of the beam, with sampling frequency 100 Hz and sensing space 2.56 mm. Two damage scenarios are performed by placing the magnetics at two different locations (285mm left and 1170mm left respectively). A small range 38-42 Hz around the 1st resonant frequency is chosen to estimate the damage features. Since sampling frequency is 100 Hz, the maximum frequency component can be observed at 50 Hz. Within the frequency range of 0-50 Hz, only the first strain mode is correctly acquired. Along this 2m single fiber optic, 100 strain sensors with nearly 15 mm spacing are chosen. Fig. 12 shows the autospectrum of the 100 strain sensing measurement points for intact beam.

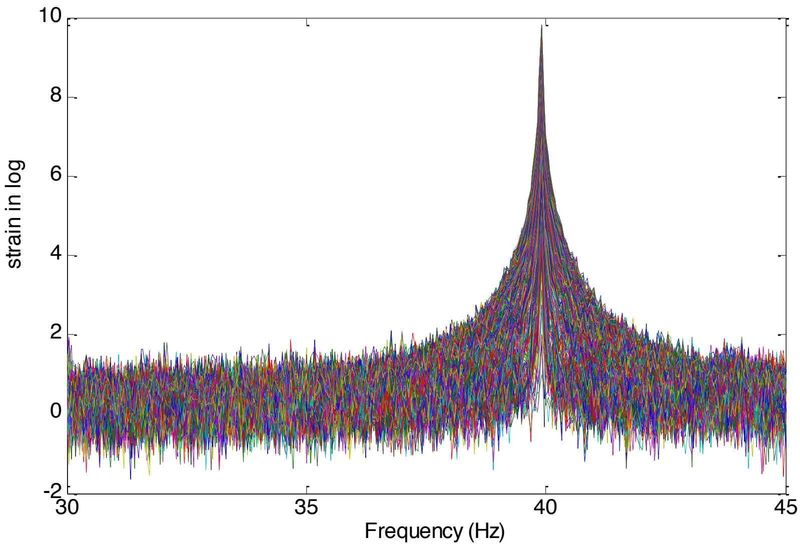

Fig. 12 Autospectrum from 100 fiber optic sensors for intact beam

The first scenario is adding magnetics on the left side of the beam.

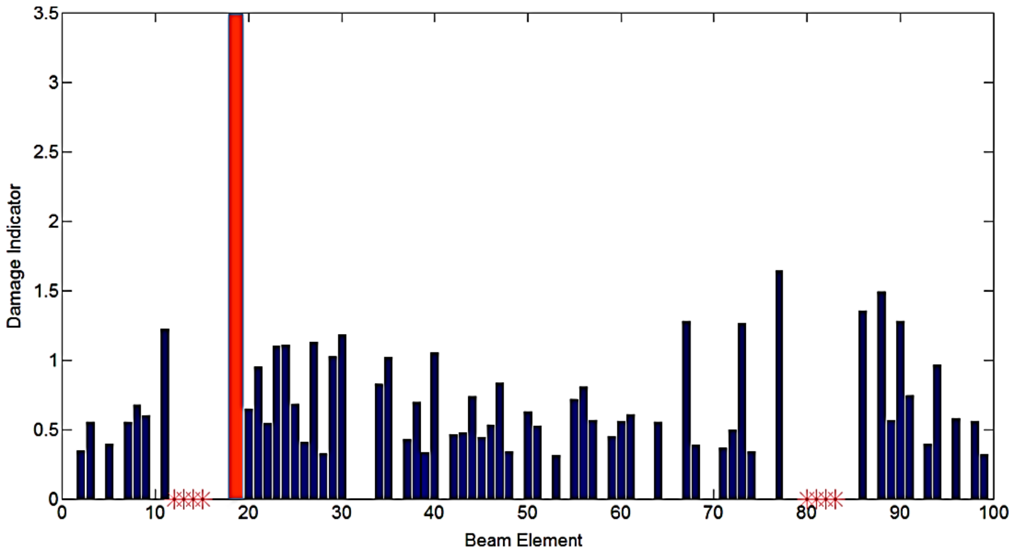

Fig. 13 Damage indicator of scenario 1

In Fig. 13, red bar revealed the damage location at 19th beam element based on the damage index from equation (3) which is in accordance with the true location of additional magnets at 285mm. Seemingly to simulations, the damage indicator in 19th element is prominent in comparison with others, which is easy to be recognized as damage component.

Occurrence damage feature has been taken into consideration as well and the identification result is shown in Fig. 14. Apparently, occurrence shows a clear recognition of the damage element in contrast with damage indicator of Fig. 13. Only one nonzero value can be seen at the 19th beam element where the magnets are placed.

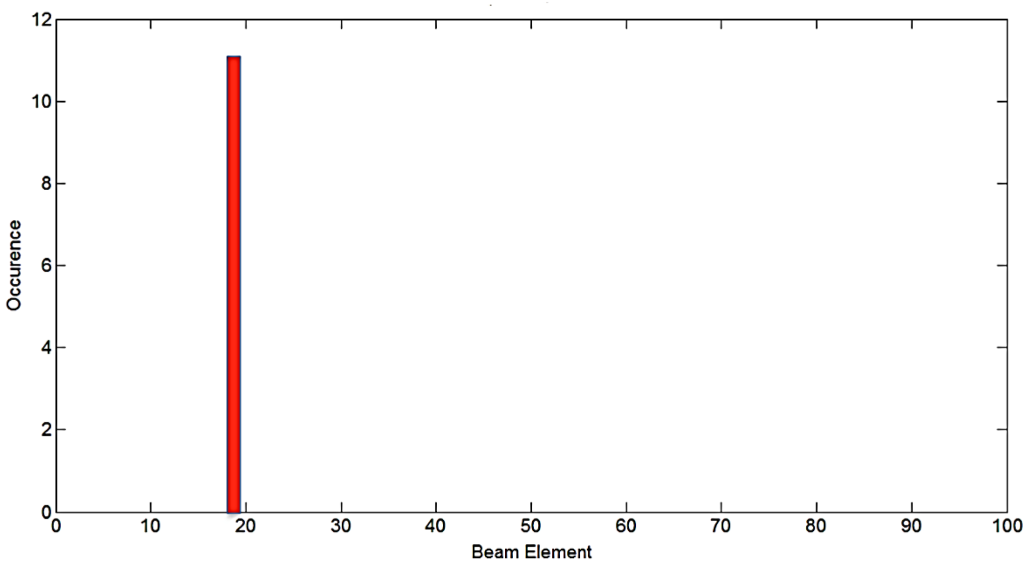

Fig. 14 Occurrence of scenario 1

Scenario two is made by adding magnetics on the right side of the beam.

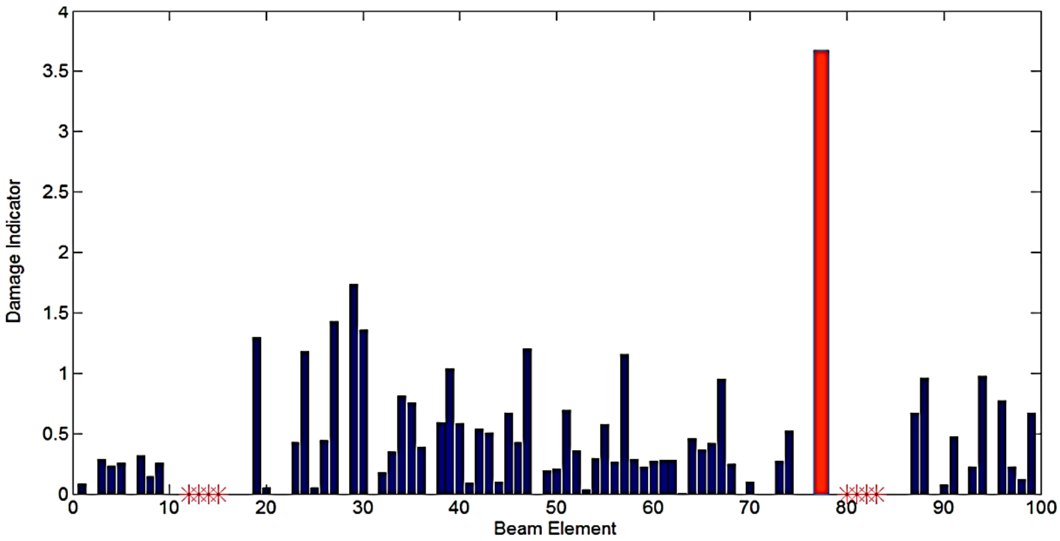

Fig. 15 Damage indicator of scenario 2

In scenario 2, red bar indicates the location of additional magnets which appears at 78th beam element in Fig. 15. The damage identification result is in correspondence of the true location where the magnets are placed. Fig. 16 shows the result of occurrence that points out correctly the damage location. Even though there are two small non-zero values at element 19th and element 67th but they can be neglected compared to element 78th.

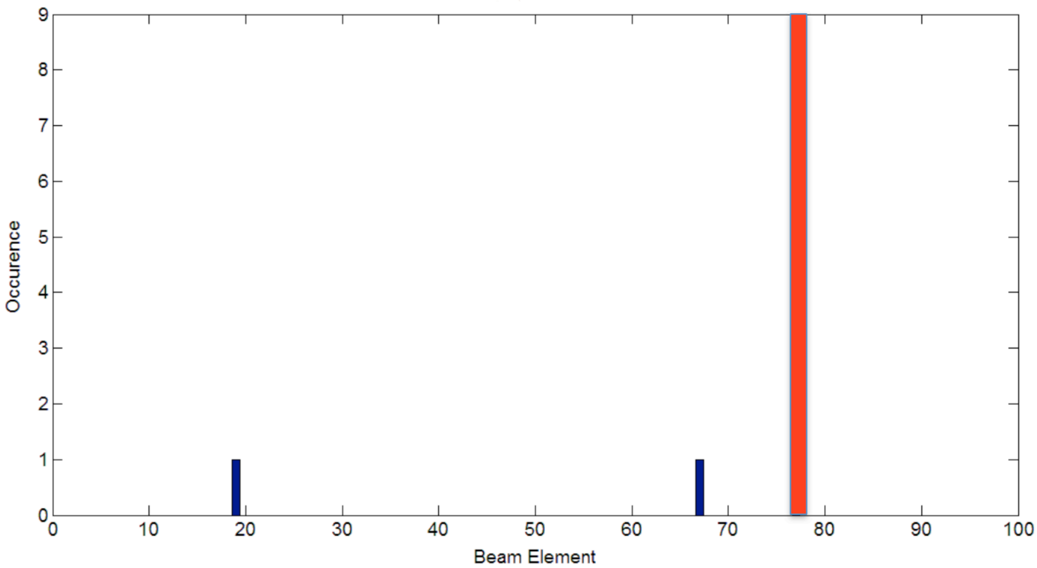

Fig. 16 Occurrence of scenario 2

Asterisks marked in Fig. 13 and Fig. 15 indicate the area where the damage feature is unreliable. This is due to the fact that those sensing points along the fiber are inside the area of strain nodes for the 1st strain mode which is basically equal to the curvature of the 1st mode shape of a clamped-clamped beam.

Transmissibility coherence function has been calculated in order to discard the unreliable damage indicators. It can be defined as follows:

$$C_{T_i^\varepsilon,T_{i+1}^\varepsilon}(f)=\frac{\left|G_{T_i^\varepsilon,T_{i+1}^\varepsilon}(f)\right|^2}{G_{T_i^\varepsilon,T_i^\varepsilon}(f)G_{T_{i+1}^\varepsilon,T_{i+1}^\varepsilon}(f)} \tag{15}$$

Where $G_{T_i^\varepsilon,T_{i+1}^\varepsilon}(f)$ the cross spectral density between *i*th STF and *i+1*th STF, $G_{T_i^\varepsilon,T_i^\varepsilon}(f)$and $G_{T_{i+1}^\varepsilon,T_{i+1}^\varepsilon}(f)$ are auto spectral density of *i*th STF and *i+1*th STF respectively. The value of $G_{T_i^\varepsilon,T_{i+1}^\varepsilon}(f)$ is always between 0 and 1 which reflects the extent of linearity between two consecutive nodes.

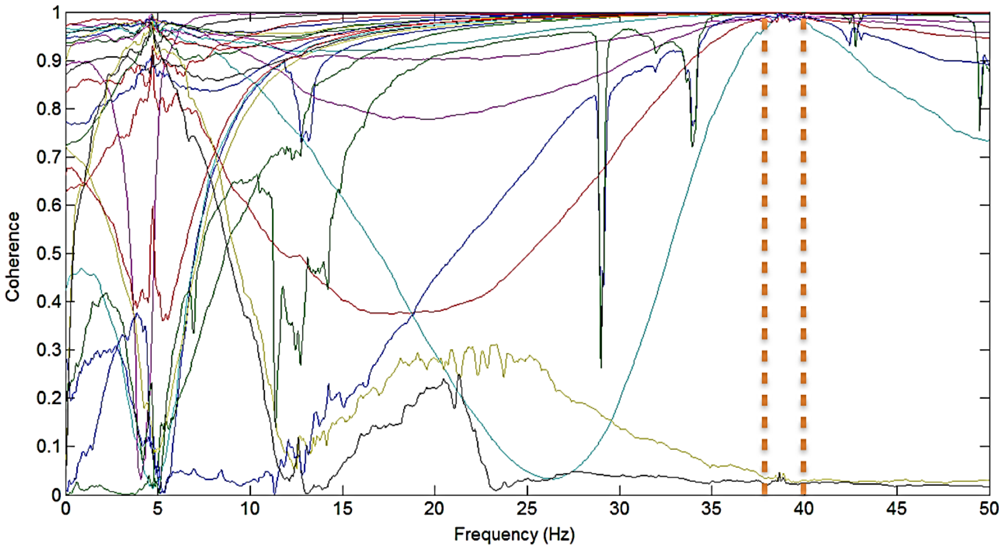

Fig. 17 Strain transmissibility coherence function

Fig. 17shows the result of coherence function among the points used to estimate the transmissibility function. In this figure, 25 beam elements (sensors) have been selected evenly from the entire 100 sensors and corresponding strain transmissibility coherence functions have been calculated. The 1st resonance frequency is located in the area between two dash lines. In order to discard the unreliable ones, threshold for coherence function is set as 0.9. If the coherence values are closer to 1 means the corresponding STFs are reliable. Since we are interested in the area around resonance frequency, it is easy to observe that there are two coherence functions under the threshold 0.9, actually lower than 0.1. Hence, these two corresponding damage indicators should be discarded. This gives an explanation for the results of Fig.18 where the sensors placed near or at strain mode nodes are flagged as unreliable data.

6. Conclusion

In this paper, strain transmissibility function is applied to damage identification simulated by adding mass to a beam structure into one point. Based on the fact that the limit value of STFs into system poles is equal to the ratio of strain mode, which are more sensitive to damage than displacement modes, these damage features based on STF reveal to have good sensitivity to damage. Both simulation and experiment illustrate the feasibility and effectiveness of using STFs to damage identification. Concerning about the future work needed to be finished, more damage scenarios should be introduced into the structure that not only adding mass but cracks which can be regarded as nonlinear damage. More complicated structures should be testified by using STFs as well.

7. Funding

This study is supported by China Scholarship Council grant.

8. References

1. Jean-Jacques Sinou. A review of damage detection and health monitoring of mechanical systems from changes in the measurement of linear and non-linear vibrations. Robert C. Sapri. Mechanical Vibrations: Measurement, Effects and Control, Nova Science Publishers, Inc., pp.643-702, 2009, 978-1-60692-037-4.

2. Aditi Majumdar, Bharadwaj Nanda, Dipak Kumar Maiti, and Damodar Maity, "Structural Damage Detection Based on Modal Parameters Using Continuous Ant Colony Optimization," Advances in Civil Engineering, vol. 2014, Article ID 174185, 14 pages, 2014. doi:10.1155/2014/174185.

3. S. W. Doebling, C. R. Farrar, and M. B. Prime, "A summary review of vibration-based damage identification methods," Shock and Vibration Digest, vol. 30, no. 2, pp. 91–105, 1998.

4. W. Fan and P. Qiao, "Vibration-based damage identification methods: a review and comparative study," Structural Health Monitoring, vol. 10, no. 1, pp. 83–111, 2011.

5. Wenxin Ren and Zhouhong Zong, Output-only modal parameter identification of civil engineering structures. Structural Engineering and Mechanics, Vol. 17, No. 3-4 (2004).

6. Q. Chen, Y.W. Chan, K. Worden, G.R. Tomlinson, Structural fault detection using neural networks trained on transmissibility functions, in: Proceedings of the International Conference on Vibration Engineering, Beijing, China, 1994, pp 456–646.

7. R. C. SAMPAIO, N. M. M. MAIA, A. M. R. RIBEIRO and J. M. M. SILVA, Damage detection using the transmissibility concept. Proceedings of the 6th International Congress on Sound and vibration, pp. 2559-2568, Copenhagen, Denmark (1999).

8. N.M.M. Maia, A.M.R. Ribeiro, M. Fontul, D. Montalvão, R.P.C. Sampaio, "Using the Detection and Relative Damage Quantification Indicator (DRQ) with Transmissibility", Key Engineering Materials, Vol. 347, pp. 455-460, 2007.

9. W. Liu, D.J. Ewins, Transmissibility properties of MDOF systems, in: Proceedings of the International Modal Analysis Conference No16, Santa Barbara CA, USA, 1998, pp. 847–854.

10. S. Ribeiro a. On the generalisation of the transmissibility concept. Mech. Syst. Signal Process., 14 (1) (2000), pp. 29–35.

11. N.M.M. Maia. The transmissibility concept in multi-degree-of-freedom systems Mech. Syst. Signal Process., 15 (1) (2001), pp. 129–137.

12. Xueyan Zhao, Ziqiang Lang.etc. A New Transmissibility Analysis Method for Detection and Location of Damage via Nonlinear Features in MDOF Structural Systems. IEEE/ASME Transactions on Mechatronics (Volume:20 , Issue: 4) ,1933 – 1947, 2015.

13. Z. Q. Lang, G. Park, C. R. Farrar, M. D. Todd, Z. Mao, L. Zhao, and K. Worden, "Transmissibility of non-linear output frequency response functions with application in detection and location of damage in MDOF structural systems," Int. J. Nonlinear Mech., vol. 46, no. 6, pp. 841–853, 2011.

14. Z. Q. Lang and S. A. Billings, "Output frequency characteristics of nonlinear systems," Int. J. Control., vol. 64, no. 6, pp. 1049–1067, 1996.

15. Yi, X., Zhu, D., Wang, Y., Guo, J., Lee, K.-M. Transmissibility-function-based structural damage detection with tetherless mobile sensors (2010) Bridge Maintenance, Safety, Management and Life-Cycle Optimization - Proceedings of the 5th International Conference on Bridge Maintenance, Safety and Management, pp. 328-335.

16. Siebel, T. & Mayer, D. (2011). Damage Detection on a Truss Structure using Transmissibility Functions, Eurodyn 2011, Leuven, Belgium.

17. C. Devriendt and P. Guillaume, Identification of modal parameters from transmissibility measurements Journal of Sound and Vibration 314(Issue 1–2) (2007), 343–356.

18. Devriendt, C., Presezniak, F., De Sitter, G., Vanbrabant, K., De Troyer, T., Vanlanduit, S., Guillaume, P. Structural health monitoring in changing operational conditions using tranmissibility measurements (2010) Shock and Vibration, 17 (4-5), pp. 651-675.

19. Whalen, T.M. The behavior of higher order mode shape derivatives in damaged, beam-like structures (2008) Journal of Sound and Vibration, 309 (3-5), pp. 426-464.

20. Chesné, S., Deraemaeker, A. Damage localization using transmissibility functions: A critical review (2013) Mechanical Systems and Signal Processing, 38 (2), pp. 569-584.

21. Measures, R.M. Structural Monitoring with Fiber Optic Technology; Academic Press: San Diego, CA, USA, 2001; Chapter 2.

22. Bao, X., Chen, L. Recent Progress in Distributed Fiber Optic Sensors (2012) Sensors (Switzerland), 12 (7), pp. 8601-8639.

23. Hotate, K. Distributed fiber sensing Technology: Currents and Challenges (2012) Optica Pura y Aplicada, 45 (2), pp. 63-69.